Applied Surface Science
Volume 254, Issue 8, 15 February 2008, Pages 2493–2498

Superhydrophobic properties of silver-coated films on copper surface by galvanic exchange reaction

A. Safaee,
D.K. Sarkar,
M. Farzaneh
Industrial Chair on Atmospheric Icing of Power Network Equipment (CIGELE1) and Canada Research Chair on Atmospheric Icing Engineering of Power Networks (INGIVRE), Université du Québec à Chicoutimi (UQAC), 555 Boulevard de l'Université, Chicoutimi, Québec, Canada G7H 2B1

Received 13 August 2007, Revised 14 September 2007, Accepted 25 September 2007, Available online 1 October 2007
doi:10.1016/j.apsusc.2007.09.073

Abstract

Hydrophobic properties of thin nanostructured silver films produced by galvanic exchange reaction on a copper surface were studied after passivation with stearic acid. The morphology of the silver films was controlled by varying the concentration of silver nitrate in the solution. Water contact angle as high as 156° and contact angle hysteresis as low as 5° were achieved for samples obtained with initial silver ion concentration of 24.75 mM in the solution. However, a strong dependence of contact angle and contact angle hysteresis on the fractal-like morphology of the silver films was observed with the variation of silver ion concentration.

Keywords : Superhydrophobicity; Microstructure; Electron microscopy; Galvanic exchange reaction

---

1. Introduction

Superhydrophobicity is currently the focus of considerable research because of its scientific and technological importance [1], [2], [3], [4], [5] and [6]. Many plants and insects feature surface microstructures covered with waxy tissues which make them superhydrophobic, i.e. with surface contact angle of water greater than 150° and where water drops roll off easily even with the slightest inclination. This special behavior is called the “lotus effect” [7]. As the basic electrostatic interactions at water/solid and ice/solid interfaces remain the same, superhydrophobic surfaces have potential to be icephobic, i.e. to reduce adhesion strength at ice/solid or snow/solid interfaces [8] and [9].

Since the water–solid interactions are limited to the outermost layers of solid surfaces, it is possible to mimic the lotus effect by altering the chemical and morphological properties of surfaces [10], [11] and [12]. In view of rendering a surface superhydrophobic, many strategies have been investigated to control the shapes, dimensions and regularity of the surface patterns using several methods which include photolithography [13], sol–gel [14] and [15], plasma etching [16], and chemical etching [17] and [18].

Electrochemistry has been used extensively for the formation of nanostructured surfaces, either by applying certain external potential between the electrodes [19], [20], [21] and [22] or simply by making use of the galvanic ion exchange reaction (without external potential) between a substrate and ions [23], [24], [25] and [26]. These methods have also been used to produce superhydrophobic surfaces after passivation with a monolayer of n-dodecanethiol [17], [25] and [26]. In particular, superhydrophobic behavior has been reported on a copper substrate with the formation of urchin-like copper phosphate dehydrate structures prepared by galvanic cell corrosion [25]. Particularly, the galvanic exchange reaction has been used to create superhydrophobic fractal-like gold nanostructured films on silicon surfaces [26]. Similarly, this method has been used to create silver nanostructured films on silicon surfaces [27] and the superhydrophobicity of such films has been reported as well [28].

In this paper, it is reported that superhydrophobicity of nanostructured silver films was achieved by galvanic exchange reaction on copper surfaces after passivation with stearic acid (SA) molecules. The properties of these surfaces are discussed through measuring the contact angle of water and characterizing their surface topography by scanning electron microscopy.

2. Experimental procedures

One-inch-square copper substrates were ultrasonically cleaned in potassium hydroxide solution then rinsed in deionized water. The coatings of thin silver films were performed by immersing the copper substrates in a silver nitrate solution for a range of time. These samples were passivated with SA dissolved in acetone or hexane (2 mM) for 30 min then dried in an oven at 80 °C overnight. The stability of SA passivation was investigated by immersing the passivated samples in water or some organic solvents such as ethanol, acetone and hexane for 12 h, followed by drying for more than 10 h in the oven. Smooth silver films were grown on silicon wafer by a thermal evaporation technique with 0.2 nm/sec deposition rate up to a thickness of 40 nm. After drying, the silver-coated samples were passivated with the method mentioned above. The surface morphology of the copper samples was studied with a field emission scanning electron microscope (FESEM, Leo 1525), whereas the silicon samples were observed with an atomic force microscope (tapping mode, VEECO, IIIa). The water contact angle measurements were made with the sessile drop method using a Krüss DSA100 drop shape analyzer.

3. Results and discussion

It is well known that copper can reduce silver ions spontaneously as described by the following reaction:

Equation (1)

$$2Ag^+ + Cu \rightarrow 2Ag + Cu^{2+}$$

Several thin silver films were coated on copper substrates by placing them in a silver nitrate solution involving this reaction (1). The passivation process is done using SA dissolved in acetone or hexane. It is known that SA molecules are chemisorbed on silver as carboxylate with its two oxygen atoms bound symmetrically to the surface [29]. No difference in water contact angle was detected according to the type of solvent. Fig. 1 depicts the variation of contact angle and hysteresis over a range of coating times for three values of initial Ag^+ concentrations of 13.2, 24.75 and 50 mM. With the 3.2 mM solution, contact angle increases monotonically from 134° at 0.5 min to 150° at 10 min, and finally to 151° after 12 h, while hysteresis correspondingly reduces from 29.5° at 1 min to 7.6° at 10 min and then to 6.5° after 12 h. On the other hand with the 50 mM solution, contact angle reduces from 155° to 147° and hysteresis increases from 5.1° to 10.3° at 0.5 and 10 min, respectively. Using the 24.75 mM solution, the highest contact angle, 156°, is obtained at 1 min while the least hysteresis, 4.1°, is achieved at 2 min.

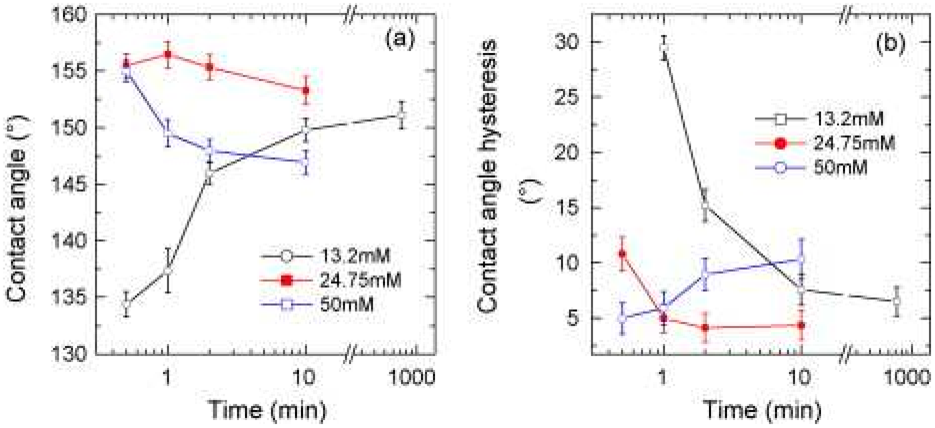

Fig. 1.

Variation of water contact angle and hysteresis with coating time.

Fig. 2 shows the water contact angle and its hysteresis for samples prepared at 1-min coating time within a range of silver ion concentrations. Increasing the Ag+ concentration from 13.2 to 396 mM increases contact angle from 137° to its maximum of 156° at 24.75 mM, and then decreases it to 141°. On the other hand, hysteresis reduces from 29.5° to 5° at 24.75 mM, and then increases to 15.5°. At higher concentrations the surface of coating is quite non-uniform and the errors in the measured contact angle and hysteresis are much higher.

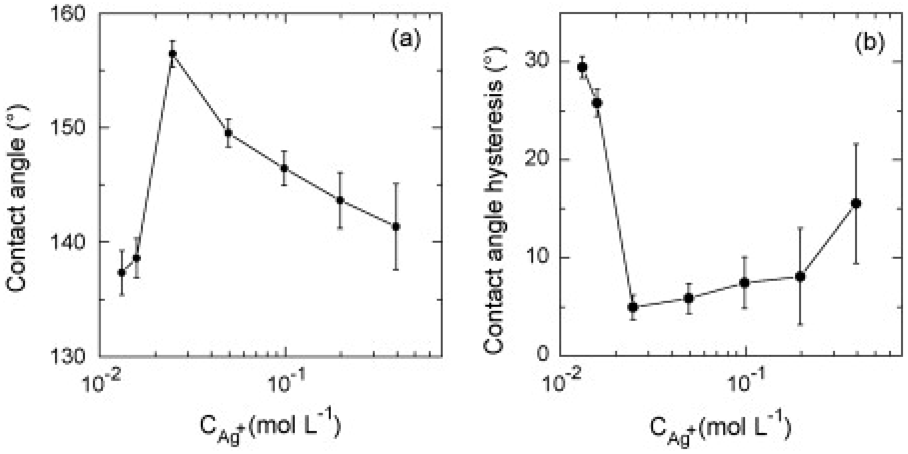

Fig. 2.

Variation of water contact angle (a) and hysteresis (b) with the initial Ag+ concentrations.

Fig. 3(a)–(c) show the SEM images of samples prepared using three different initial Ag+ concentrations of 13.2, 24.75 and 396 mM, respectively. It can be seen that the size and number of both the fractal-like structures and the voids surrounded by them are concentration-dependent. Because of the low Ag+ concentration, the reaction is slow and the film has tiny, almost indistinguishable voids, as shown in Fig. 3(a). After SA passivation, this sample shows a water contact angle and a contact angle hysteresis of 137° and 29.5°, respectively, as shown in the inset of Fig. 3(a). When the initial Ag+ concentration is increased, the reaction becomes faster and larger fractal-like structures of silver appear. Consequently, the size of the voids between those structures also increases. The average diameter of the voids is ~5 μm, as shown in Fig. 3(b). The contact angle and contact angle hysteresis obtained are 156° and 5°, respectively, as shown in the inset of Fig. 3(b). By further increasing the concentration of Ag+ ions in the solution, the size of the voids increases to ~10 μm, as seen in Fig. 3(c) and the contact angle and hysteresis are 141° and 15.5°, respectively, illustrated in the inset of Fig. 3(c). Fig. 3(d) depicts a magnified fractal-like structure from Fig. 3(b). Due to their self-similarity, several nanometric empty spaces exist around the micrometric structures which are separated by voids.

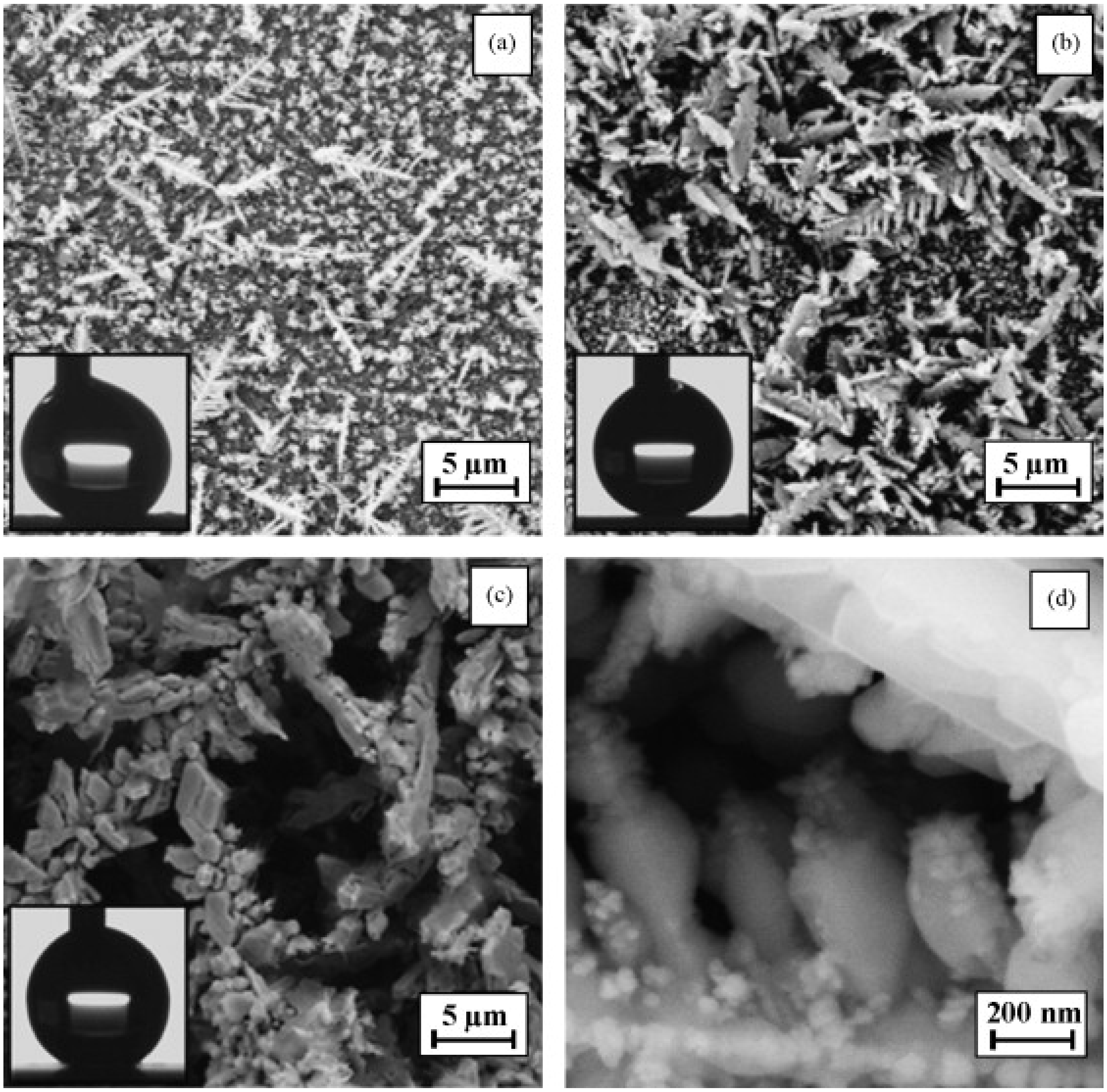

Fig. 3.

SEM images of samples prepared using three different initial Ag+ concentrations of (a), 13.2 mM, (b) 24.75 mM and (c) 396 mM, respectively; and (d) a magnified section of (b). In the insets, the states of the droplets are shown.

To fully understand the superhydrophobicity of the surface of the Ag-aggregate-coated copper samples, the contact angles can be studied as follows: the water contact angle on rough surfaces is commonly explained with two models, namely Wenzel [30] and Cassie–Baxter [31] models. In the Wenzel model [30] the contact angle is given by

Equation (2)

$\cos \theta' = r \cos$

where r is the roughness factor defined as the ratio of the actual area of a rough surface to the projected area, θ is the contact angle on the corresponding smooth surface and θ′ is that of the rough surface. Since r is greater than 1 due to roughness, then θ′ < 90° if θ < 90° and θ′ > 90° if θ > 90°. On the other hand, the modified Cassie–Baxter model [32] and [33] predicts the equilibrium contact angle as

Equation (3)

$\cos\theta' = f(1+\cos\theta) -$

where f is the fraction of solid surface area in contact with the water drop and remaining area (1−f) is occupied by air for which the contact angle of water is 180°. With this model, it is possible to obtain θ′ > 90° even if θ < 90°, provided that f is very small, which is achievable by means of fractal structures [34], by a bottom-up approach [35] or even by highly ordered surface by photolithography [13].

A smooth thin film of silver was prepared on silicon (1 0 0) wafer and its morphology was observed with AFM. From the AFM images, one can see that the Ag layer is flat and homogenous, as shown in Fig. 4. For the sample of Fig. 4 with 2 μm scan length, the measured RMS roughness is determined to have a maximum value of 1.08 nm. With this value, it is assumed that the surface is smooth and can be used for evaluating water contact angle on smooth silver.

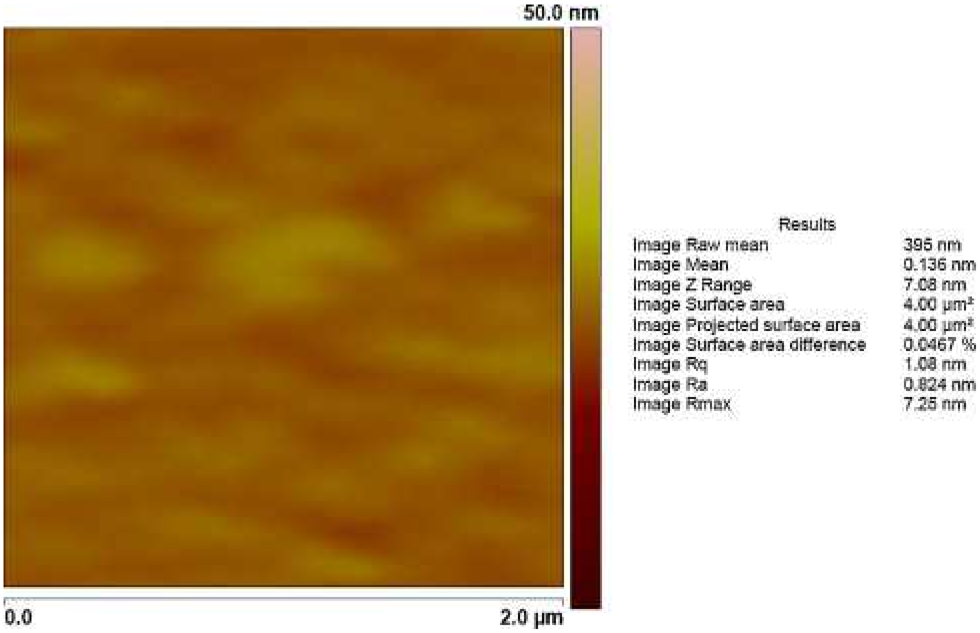

Results

Image Raw mean	395 nm
Image Mean	0.136 nm
Image Z Range	7.08 nm
Image Surface area	4.00 μm²
Image Projected surface area	4.00 μm²
Image Surface area difference	0.0467 %
Image Rq	1.08 nm
Image Ra	0.824 nm
Image Rmax	7.25 nm

Fig. 4.

AFM image of the smooth silver surface and its corresponding parameters.

The surface wettability of the smooth silver was studied by contact angle measurements after passivation with SA in acetone or hexane, and no difference in water contact angles was detected according to the type of solvent. As shown in Fig. 5, the water contact angle was about 79 ± 1.1°, implying that the passivated surface is slightly hydrophilic. Although many of the reported superhydrophobic materials are based on the materials with water contact angle greater than 90° in their smooth form, it is not a necessary condition and it is possible to produce superhydrophobic surfaces using slightly hydrophilic materials [35] and [36]. In our experiment, increasing the passivation period or the concentration of SA by more than 2 mM may lead to the formation of patches of SA on the surface, detectable by AFM, which increases its roughness. In such cases, higher water contact angles may be obtained because the film which is not smooth.

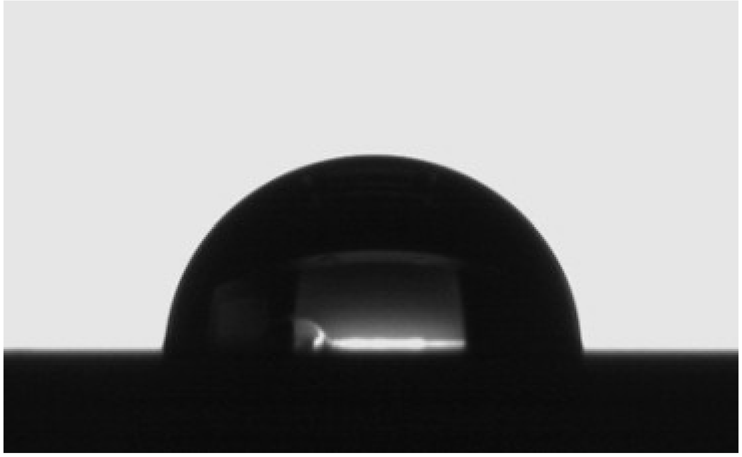

Fig. 5.

Image of a water droplet of about 6 μL on the smooth silver surface of Fig. 4, with water contact angle of 79°.

The fractions of solid surface, f, of the samples prepared with different Ag+ ion concentrations were calculated using Eq. (3) with the measured values of θ′ (137°, 156° and 141°) for the samples shown in Fig. 3(a)–(c), respectively, and considering that θ has a value of 79° for the stearic acid-passivated smooth surface. The calculated f values are found to be 0.226, 0.072 and 0.187 for the microstructures presented in Fig. 3(a)–(c), respectively. These values are comparable with the reported solid fraction values belonging to other disordered microstructures, for example, the results of Tavana et al. [37] on thermal evaporated polymer (C36H74) surface or Wang et al. [26] on branch-like structures of gold, resulting from galvanic exchange reaction. In the experiment of Tavana et al. [37], the samples have suitable roughness for AFM studies, and the experimentally achieved solid fraction was reported to be ~0.12. Our samples are highly rough and therefore inappropriate for AFM measurements to determine the f value experimentally. On the other hand, there exists a consistency between the achieved contact angles and the calculated f values in the present study on the fractal-like structures of silver (contact angle: 156° and f value: 0.072) and those on the branch-like structures of gold (contact angle: 158° and f value: 0.09) by Wang et al. [26]. The fraction of solid 0.09 has been calculated from the given air fraction of 0.904 in Table 1 by Wang et al. [26] as (1−0.904) = 0.096 ~ 0.09.

Table 1.

Water contact angle (CA) and hysteresis (CAH) of the as-prepared superhydrophobic surface and the samples treated with water or some organic solvents

Sample	CA (°)	Variation of CA (°)	CAH (°)	Variation of CAH (°)
As-prepared	156.3 ± 1.2	–	5.0 ± 1.3	–
Treated with water	155.8 ± 1.2	−0.5 ± 2.4	5.3 ± 1.1	+0.3 ± 2.4
Treated with ethanol	156.2 ± 1.4	−0.1 ± 2.6	5.2 ± 1.4	+0.2 ± 2.7
Treated with acetone	156.1 ± 1.7	−0.2 ± 2.9	5.2 ± 1.7	+0.2 ± 3.0
Treated with hexane	156.1 ± 1.7	−0.2 ± 2.9	5.2 ± 1.7	+0.2 ± 3.0

In the experiment of Wang et al. [26], the best hydrophobicity was achieved with the HAuCl4 reagent with concentration equal to 25 mM. Comparing their experiment with this work, there is not only a qualitative similarity in the morphology of fractal-like nanostructures, but also a quantitative similarity in initial reagent concentrations (24.75 mM AgNO3 versus 25 mM HAuCl4). However, the fractal-like nanostructures of silver have smaller solid fraction (f = 0.072) compared with the branch-like structures of gold (f = 0.09).

The stability of superhydrophobicity of the SA-passivated fractal-like silver nanostructured surfaces (24.75 mM, 1 min) was verified by immersing them in water and different organic solvents, namely ethanol, acetone and hexane, prior to performing the contact angle measurements. Fig. 6 and Table 1 show the measured values of water contact angle and hysteresis. The as-prepared SA-passivated surfaces have contact angle and hysteresis of 156.3 ± 1.2° and 5.0 ± 1.3°, respectively. After immersion in water, these values change to 155.8 ± 1.2° and 5.3 ± 1.1°, respectively, which are very close to those of the as-prepared surfaces. As a whole, the variations of contact angle and hysteresis are found to be less than 0.5° and 0.3°, respectively, after treating with either water or organic solvents of ethanol, acetone and hexane. These results suggest that SA-passivated fractal-like silver nanostructured surfaces are very stable with respect to treating with water and organic solvents.

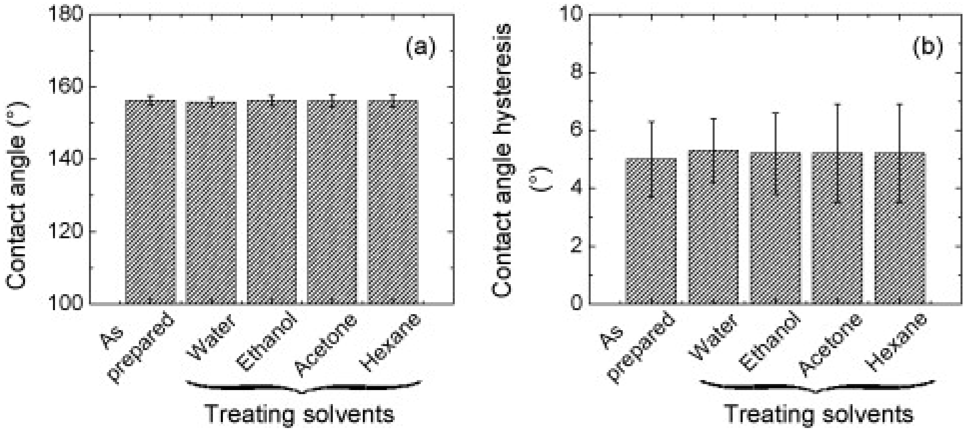

Fig. 6.

Variation of water contact angle and hysteresis after treating the passivated samples with water or organic solvents of ethanol, acetone or hexane.

4. Conclusion

In this study, a simple procedure to produce stable superhydrophobic surfaces with contact angles as high as 156° and contact angle hysteresis as low as 5°, is proposed. It makes use of the galvanic ion exchange reaction between silver ions with copper on the surface, and of passivation with stearic acid organic molecules. Microstructures of silver-coated samples are composed of fractal-like structures, as well as voids surrounded by fractals. The optimum void size of ~5 μm leads to the maximum contact angle and minimum contact angle hysteresis. These superhydrophobic nanostructured surfaces are found to be resistant to water and organic solvents.

Acknowledgements

This work was carried out within the framework of the NSERC/Hydro-Quebec/UQAC Industrial Chair on Atmospheric Icing of Power Network Equipment (CIGELE) and the Canada Research Chair on Engineering of Power Network Atmospheric Icing (INGIVRE) at Université du Québec à Chicoutimi. The authors would like to thank the CIGELE partners (Hydro-Québec, Hydro One, Électricité de France, Alcan Cable, K-Line Insulators, CQRDA and FUQAC) whose financial support made this research possible. They would also like to thank Ms. Hélène Grégoire, CNRC Chicoutimi for providing access to FESEM and Mr. Jian Hung Lin, Advanced Material Laboratory, Center for Condensed Matter Sciences, National Taiwan University, Taipei, Taiwan, for preparing smooth silver-coated silicon samples.

References

[1] B. Bhushan, Y.C. Jung
Ultramicroscopy, 107 (2007), p. 1033
[2] Z. Guo, J. Fang, L. Wang, W. Liu
Thin Solid Films, 515 (2007), p. 7190
[3] A. Satyaprasad, V. Jain, S.K. Nema
Appl. Surf. Sci., 253 (2007), p. 5462
[4] A. Egatz-Gómez, S. Melle, A.A. García, S.A. Lindsay, M. Márquez, P. Domínguez-García, M.A. Rubio, S.T. Picraux, J.L. Taraci, T. Clement, D. Yang, M.A. Hayes, D. Gust
Appl. Phys. Lett., 89 (2006), p. 034106
[5] D. Quéré
Nat. Mater., 1 (2002), p. 14
[6] H.Y. Erbil, A.L. Demirel, Y. Yonca, O. Mert
Science, 299 (2003), p. 1377
[7] W. Barthlott, C. Neinhuis
Planta, 202 (1997), p. 1
[8] T. Kako, A. Nakajima, H. Irie, Z. Kato, Z. Uematsu, T. Watanabe
J. Mater. Sci., 39 (2004), p. 547
[9] S.A. Kulinich, M. Farzaneh
Appl. Surf. Sci., 230 (2004), p. 232
[10] L. Feng, S. Li, Y. Li, H. Li, L. Zhang, J. Zhai, Y. Song, B. Liu, L. Jiang, D. Zhu

Adv. Mater., 14 (2002), p. 1857

[11] Z.Z. Gu, H. Uetsuka, K. Takahashi, R. Nakajima, H. Onishi, A. Fujishima, O. Sato

Angew. Chem. Int. Ed., 42 (2003), p. 894

[12] S.A. Kulinich, M. Farzaneh

Vacuum, 79 (2005), p. 255

[13] D. Öner, T.J. McCarthy

Langmuir, 16 (2000), p. 7777

[14] K. Satoh, H. Nakazumi

J. Sol–Gel Sci. Technol., 27 (2003), p. 327

[15] N.J. Shirtcliffe, G. McHale, M.I. Newton, C.C. Perry, P. Roach

Mater. Chem. Phys., 103 (2007), p. 112

[16] R. Olde, J.G.A. Terlingen, G.H.M. Engbers, J. Feijen

Langmuir, 15 (1999), p. 4847

[17] N.J. Shirtcliffe, G. McHale, M.I. Newton, C.C. Perry

Langmuir, 21 (2005), p. 937

[18] D.K. Sarkar, M. Farzaneh

Proceedings of the 2006 NSTI Nanotechnology Conference and Trade Show, vol. 3, Boston, MA, USA (2006), p. 166

[19] J. Zhang, Y. Mo, M.B. Vukmirovic, R. Klie, K. Sasaki, R.R. Adzic

J. Phys. Chem. B, 108 (2004), p. 10955

[20] D.K. Sarkar, X.J. Zhou, A. Tannous, K.T. Leung

J. Phys. Chem. B. (Lett.), 107 (2003), p. 2879

[21] D.K. Sarkar, X.J. Zhou, A. Tannous, M. Louie, K.T. Leung

Solid State Commun., 125 (2003), p. 365

[22] N. Zhao, F. Shi, Z. Wang, X. Zhang

Langmuir, 21 (2005), p. 4713

[23] X.H. Xia, C.M.A. Ashruf, P.J. French, J.J. Kelly

Chem. Mater., 12 (2000), p. 1671

[24] S.J. Huo, X.K. Xue, Q.X. Li, S.F. Xu, W.B. Cai

J. Phys. Chem. B, 110 (2006), p. 25721

[25] X. Wu, G. Shi

Nanotechnology, 16 (2005), p. 2056

[26] C. Wang, Y. Song, J. Zhao, X. Xia

Surf. Sci., 600 (2006), p. L38

[27] Y.Y. Song, Z.D. Gao, J.J. Kelly, X.H. Xia

Electrochem. Solid State Lett., 8 (2005), p. C148

[28] F. Shi, Y. Song, J. Niu, X. Xia, Z. Wang, X. Zhang

Chem. Mater., 18 (2006), p. 1365

[29] S.J. Lee, K. Kim

Vib. Spectrosc., 18 (1998), p. 187

[30] R.N. Wenzel

Ind. Eng. Chem., 28 (1936), p. 988

[31] A.B.D. Cassie, S. Baxter

Trans. Faraday Soc., 40 (1944), p. 546

[32] J. Bico, C. Marzolin, D. Quéré

Europhys. Lett., 47 (1999), p. 220

[33] A. Nakajima, K. Hashimoto, T. Watanabe

Monatshefte für Chemie, 132 (2001), p. 31

[34] S. Shibuichi, T. Onda, N. Satoh, Kaoru Tsujii

J. Phys. Chem., 100 (1996), p. 19512

[35] E. Hosono, S. Fujihara, I. Honma, H. Zhou

J. Am. Chem. Soc., 127 (2005), p. 13458

[36] N.J. Shirtcliffe, S.A. Aqil, C. Evans, G. McHale, M.I. Newton, C.C. Perry, P. RoachJ

Micromech. Microeng., 14 (2004), p. 1384

[37] H. Tavana, A. Amirfazli, A.W. Neumann

Langmuir, 22 (2006), p. 5556